

ORIGINAL ARTICLE

Tumor-associated soluble uPAR-directed endothelial cell motility and tumor angiogenesis

JS Rao^{1,2}, M Gujrati³ and C Chetty¹

The expression of urokinase-type plasminogen activator (uPA) receptor (uPAR) correlates with the malignant phenotype of various cancers. The soluble form of uPAR (s-uPAR) is present in the circulation of cancer patients, but the role of s-uPAR in endothelial cell migration is poorly understood. Therefore, we examined the role of tumor-associated s-uPAR on endothelial cell motility and angiogenesis. Here, we present evidence that tumor-associated s-uPAR augments the migration of human umbilical vein endothelial cells (HUVECs). When grown on tumor-conditioned medium, the membrane fraction of HUVECs had increased localization of s-uPAR onto its cell membrane. Colocalization studies for GM1 ganglioside receptor and uPAR further demonstrated s-uPAR recruitment onto lipid rafts of HUVECs. Immunoblot analysis for uPAR in lipid raft fractions confirmed s-uPAR recruiting onto HUVECs' membrane. Further, s-uPAR induced Rac1-mediated cell migration while either function-blocking uPAR antibodies or dominant-negative mutant Rac1 expression in HUVECs-mitigated s-uPAR-enhanced cell migration. In addition, orthotopic implantation of uPAR-overexpressing cells resulted in a significant increase in circulating s-uPAR in blood serum and invasive nature of tumor and tumor vasculature in mice. Collectively, this data provide insight into tumor-associated s-uPAR-directed migration of endothelial cells and its subsequent influence on tumor angiogenesis.

Oncogenesis (2013) 2, e53; doi:10.1038/oncsis.2013.19; published online 24 June 2013

Subject Categories: Molecular oncology

Keywords: soluble uPAR; migration; angiogenesis; glioma; lipid raft

INTRODUCTION

Angiogenesis is a physiological multistep process of new blood vessel formation from pre-existing blood vessels to furnish nutrients and oxygen to rapidly growing cells and is crucial for physiological growth, tissue healing, regeneration and tumor growth.¹ Owing to lack of oxygen and other essential nutrients, tumor masses beyond 1–2 mm in diameter require angiogenesis for their survival and progressive growth. This process is regulated by a tight balance between pro- and anti-angiogenic agents, and involves a cascade of events of which the migration of capillary endothelial cells is an essential component.^{1,2} The endothelial cell motile process is directionally regulated by chemotactic, haptotactic and mechanotactic stimuli, and further involves the degradation of the extracellular matrix to enable progression of the migrating cells.³ For migration, endothelial cells need to be set free from their inherent location by losing cell–cell contacts and to be polarized to focus the newly formed proteolytic machinery at the leading edge, which is essential for the matrix degradation. Consequently, proteinases of the plasminogen system, matrix metalloproteinase system, chymase and heparanase families are thought to be important. Accordingly, inhibition of functional activity of the urokinase-type plasminogen activator (uPA) receptor (uPAR) has been shown to significantly decrease the invasive potential of endothelial cells.^{4,5}

uPAR is a glycosylphosphatidylinositor-anchored membrane protein that resides in lipid rafts, which are dynamic microdomains of the cell membrane, rich in cholesterol, sphingolipids

and glycolipids, transmembrane protein receptors, integrins and a large number of signaling molecules.^{6–8} The cell surface complex of uPA and its receptor uPAR is known to be involved in the activation of intracellular signaling events associated with cellular migration.⁹ The localization of uPA/uPAR within focal adhesions at the leading edge of migratory endothelial cells¹⁰ is believed to limit proteolysis to the immediate pericellular environment, thus promoting efficient matrix remodeling while enabling individual cell detachment and subsequent migration. Many studies have shown that inhibiting uPAR-dependent signaling suppresses endothelial cell migration and markedly suppresses angiogenesis *in vitro* and *in vivo*.^{10–13} For over a decade, much effort has been focused on determining uPAR signaling mechanisms, as uPAR is significantly expressed in many cancers, including glioma.^{5,14–17} Significant amounts of the soluble form of uPAR (s-uPAR) have been found in biological fluids of cancer patients, and these levels notably correlate with tumor malignancy.^{17–19} These observations indicate that elevated expression of uPAR in tumors, particularly in malignant cells, may be a sign of more aggressive cancers.

We have demonstrated previously that downregulation of uPAR inhibited tumor angiogenesis *in vitro* and *in vivo* in various cancers.^{13,20–23} However, it is not yet clear how tumor-associated uPAR is involved in the endothelial cell migration and induction of tumor angiogenesis. Here, we have demonstrated the role of tumor-associated s-uPAR in tumor-induced angiogenesis *in vitro* and *in vivo*. Our findings demonstrate tumor cell secreted s-uPAR recruits onto endothelial cell membrane rafts and induces

¹Department of Cancer Biology and Pharmacology, University of Illinois College of Medicine at Peoria, Peoria, IL, USA; ²Department of Neurosurgery, University of Illinois College of Medicine at Peoria, Peoria, IL, USA and ³Department of Pathology, University of Illinois College of Medicine at Peoria, Peoria, IL, USA. Correspondence: Dr C Chetty, Department of Cancer Biology and Pharmacology, University of Illinois College of Medicine at Peoria, Peoria, IL 61605, USA.

E-mail: chandram@uic.edu

Received 26 April 2013; accepted 15 May 2013

extracellular-signal-regulated kinases (ERK)/Rac1-mediated cell migration, and thereby angiogenesis.

RESULTS

Tumor-associated s-uPAR enhances HUVEC invasion and migration

As the s-uPAR has been found in the biological fluids of cancer patients and is highly correlated with malignancy,^{17–19} we postulated that tumor-associated s-uPAR might be involved in endothelial cell migration, and thereby enhance angiogenesis. To test this possibility, we developed constitutively uPAR-overexpressed (UR) 4910 and 5310 cells (Supplementary Figures S1A–B and Figures 1a and b). Consistent with our hypothesis, human umbilical vein endothelial cell (HUVEC) migration was significantly augmented in cells cultured next to 4910UR/5310UR cells as compared with cells cultured next to 4910EV/5310EV cells (Figure 1c and Supplementary Figure S1C). Likewise, s-uPAR

containing conditioned medium (CM) from 4910UR/5310UR cells (UR-CM) markedly enhanced *in vitro* invasive potential of HUVECs (Figure 1d). Next, in an *in vitro* angiogenic assay,²⁴ UR-CM elicited a strong angiogenic response and induced HUVECs to differentiate into capillary-like structures within 16 h as compared with empty vector (EV)-CM. However, cells grown on serum-free medium were just beginning to differentiate into capillaries (Figure 1e). Quantification indicated a 2.5-fold increase in cumulative vessel length in HUVECs cultured with UR-CM when compared with EV-CM (Figures 1e and f).

To further confirm that s-uPAR regulates HUVEC invasion, migration and angiogenesis, we performed appropriate assays using either uPAR small interfering RNA (siRNA)-downregulated stable cells (4910UR-Si/5310UR-Si) or CM (uPAR siRNA (UR-Si)-CM). As expected, 4910UR-Si/5310UR-Si cells repressed the migration and UR-Si-CM blocked endothelial cell invasion and microvessel morphogenesis (Figures 1a–f). In addition, recombinant human uPAR (rh-uPAR) alone induced HUVEC migration, invasion and

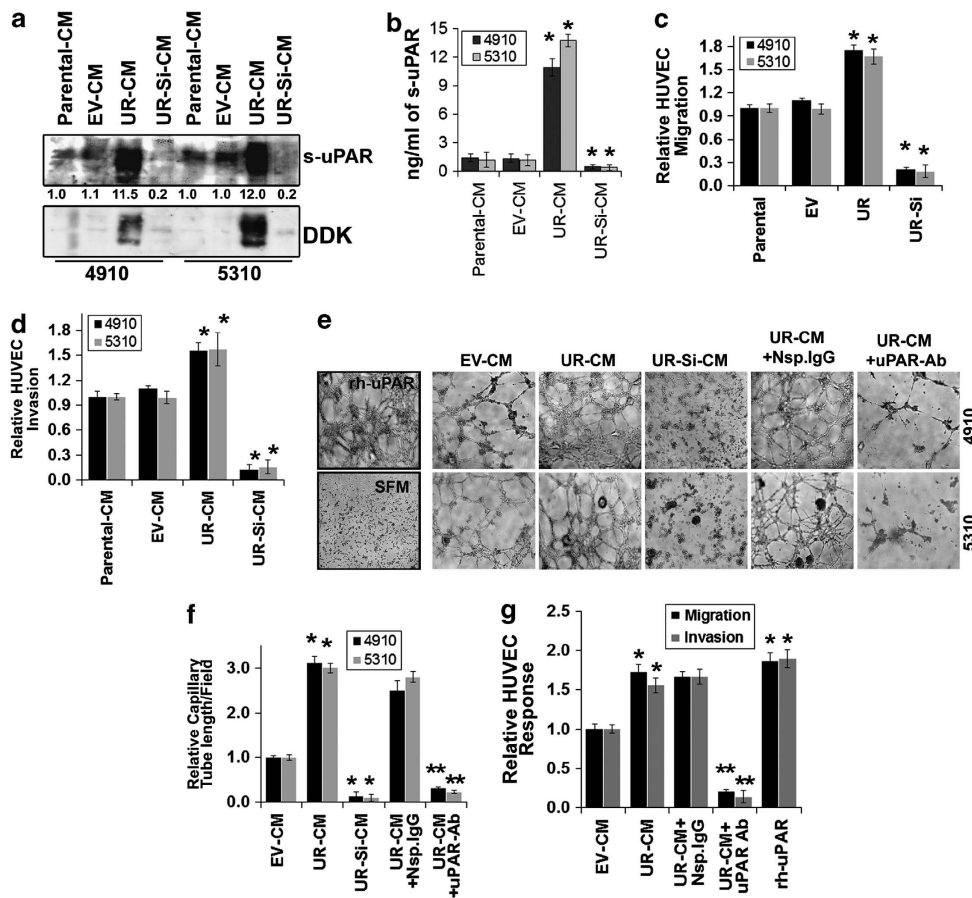


Figure 1. Tumor-associated soluble uPAR (s-uPAR) enhances HUVEC invasion, migration and angiogenesis. (a) Conditioned medium (CM) was collected from tumor cells (parental and stably expressing empty vector (EV), uPAR-cDNA (UR) and uPAR siRNA (UR-Si)). Immunoblot analyses were performed for s-uPAR and DDK using specific antibodies. (b) s-uPAR levels in CM were quantified using uPAR Quantikine Immunoassay kit. Columns: mean; bars: s.d.; $n = 3$; $*P < 0.01$ vs parental control. (c) Cells were labeled (tumor cells: Qtracker-525-Green and HUVECs: Qtracker-655-Red) and seeded into separate chambers of culture inserts. After 16 h, the culture inserts were removed and cells were allowed to migrate for a further 24 h. Images were captured at 0 and 24 h of incubation and cell migration was quantified using ImageJ software (NIH). The levels of HUVEC migration were normalized to HUVEC migration in parental cells and are represented as arbitrary units. Columns: mean; bars: s.d.; $n = 3$; $*P < 0.01$ vs parental-CM. (d) HUVEC invasion experiments were performed using ThinCertTM inserts as described in Materials and methods. The levels of HUVEC invasion was quantified and normalized to HUVEC invasion in parental-CM. Columns: mean; bars: s.d.; $n = 3$; $*P < 0.01$ vs parental-CM. (e, f) *In vitro* angiogenesis assay was performed as described in Materials and methods. The degree of angiogenic induction by CM was quantified by ImageJ software (NIH) for the numerical value of the product of the relative capillary length per microscopic field. Serum-free medium (SFM) and recombinant human uPAR (rh-uPAR) in SFM were used as controls (insets). Columns: mean; bars: s.d.; $n = 3$; $*P < 0.01$ vs parental-CM; $**P < 0.01$ vs UR-CM. uPAR antibody, uPAR-Ab; isotype control, Nsp.IgG. (g) Migration assay was performed using CM. In this case, both chambers of culture inserts were seeded with HUVECs. After 16 h, the culture inserts were removed, CM was added and cells were allowed to migrate for 24 h. Invasion assay was performed as described above. uPAR-Ab, or Nsp.IgG were added to UR-CM before adding onto cells. rh-uPAR was added to SFM. Columns: mean; bars: s.d.; $n = 3$; $*P < 0.01$ vs parental-CM; $**P < 0.01$ vs UR-CM.

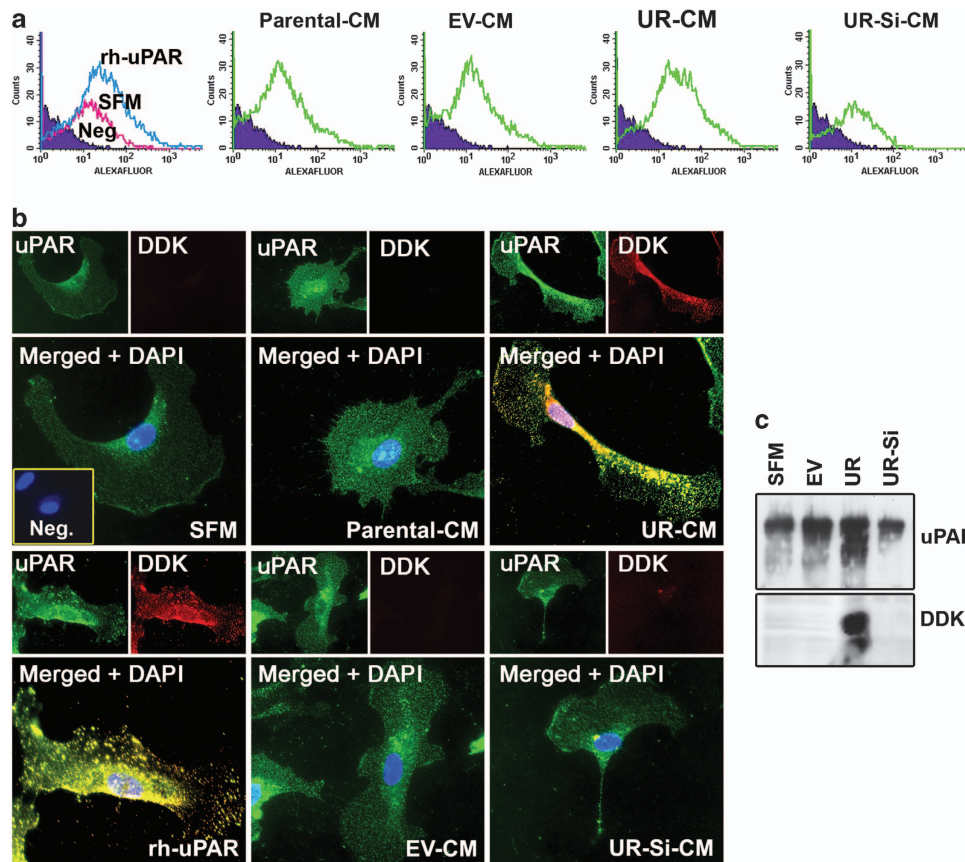


Figure 2. s-uPAR recruits onto HUVEC membrane. Conditioned medium (CM) was collected from tumor cells as described in Materials and methods. (a) HUVECs were cultured on CM for 24 h, labeled with anti-uPAR antibody, followed by Alexa Fluor-488-conjugated secondary antibody and were analyzed by fluorescence-activated cell sorting (FACS) for uPAR expression. Serum-free medium (SFM) and rh-uPAR were used as controls. Isotype control (Neg.). (b) HUVECs were cultured in chamber slides on CM for 24 h and fixed in 4% paraformaldehyde and 0.2% glutaraldehyde in phosphate-buffered saline for 1 h. Immunocytochemical analysis was performed as described in Materials and methods. Isotype control (Neg.; inset). Slides were mounted and photographed. (c) Equal amounts of proteins were used for the extraction of HUVEC membrane fractions and were subjected to immunoblot analysis for uPAR expression using specific antibodies. The blot was re-probed for DDK-tag expression.

angiogenesis, whereas supplementation of functional blocking antibodies diminished UR-CM-induced migration, invasion and angiogenesis (Figures 1e–g).

Tumor-associated s-uPAR recruits onto HUVEC membrane

To explore whether s-uPAR recruits onto membrane to induce endothelial cell migration, we cultured HUVECs on CM for 24 h and analyzed uPAR levels on the cell membrane of HUVECs using fluorescence-activated cell sorting analysis. As anticipated, the abundance of cell surface uPAR was substantially increased in HUVECs cultured in UR-CM to levels similar to those of HUVECs supplemented with rh-uPAR (Figure 2a). Next, we performed immunofluorescent microscopy for uPAR and DDK-tag (FLAG-tag/DYKDDDDK) in HUVECs cultured on CM. Colocalization of uPAR and DDK showed prominently on the cell surface, which indicates that DDK containing uPAR from UR-CM is recruiting on the HUVEC membrane (Figure 2b). This s-uPAR recruitment onto HUVEC membrane was further confirmed by the immunoblot analysis of the membrane fraction of HUVECs cultured on CM (Figure 2c).

Tumor-associated s-uPAR colocalizes in lipid rafts on HUVECs

As uPAR has been shown to colocalize in the lipid rafts of many cell types,^{6,7,21} we postulated that the tumor-associated s-uPAR also colocalizes in lipid rafts on HUVECs. Immunofluorescence co-staining of a raft marker, GM1 ganglioside receptor²⁵ and a specific anti-uPAR antibody (uPAR-Ab) showed increased amounts

of uPAR localized in the lipid rafts on cell membrane of HUVECs cultured on UR-CM similar to cells cultured with rh-uPAR (Figure 3a). To further confirm s-uPAR and raft co-clustering on cell membrane, we isolated lipid rafts from HUVECs cultured on CM²¹ and analyzed for the known raft and non-raft marker proteins²¹ (Supplementary Figures S2A and B) to confirm the relative purity of the lipid raft fractionations. Next, we analyzed lipid raft fractions for uPAR levels by immunoblot analysis. As expected, uPAR levels were markedly increased in the lipid raft fractions of HUVECs cultured on UR-CM as compared with cells cultured on EV-CM. In contrast, uPAR levels significantly decreased in the lipid raft fractions of HUVECs grown on UR-Si-CM as compared to cells grown on EV-CM (Figure 3b).

Many studies have proposed the important role of an intact lipid raft in the regulation of invasion, migration and angiogenesis.^{8,10,26} The integrity of the lipid raft depends on the concentration of cholesterol in the plasma membrane,²⁷ and methyl- β -cyclodextrin (MBCD), a chelator of cholesterol, dismantles these lipid rafts.²⁵ We therefore determined whether the disruption of lipid rafts would be able to abolish the migration, invasion and angiogenesis in HUVECs cultured on CM. MBCD treatment inhibited UR-CM-induced invasion, migration and angiogenesis (Figures 3c and d). Similarly, disruption of lipid rafts by MBCD treatment altered s-uPAR from membrane raft localization (Figures 3a and b). Collectively, these results suggest that localization of uPAR into lipid rafts' environment facilitates invasion, migration and angiogenesis action of tumor-associated s-uPAR in HUVECs.

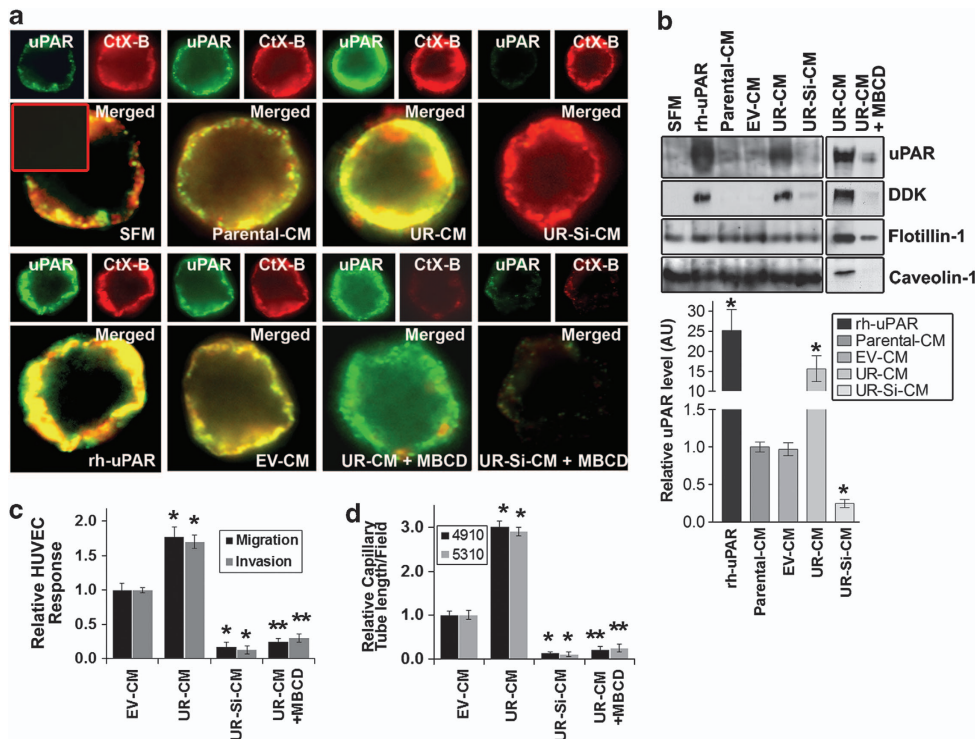


Figure 3. s-uPAR colocalizes in lipid rafts on HUVECs. Conditioned medium (CM) was collected from tumor cells as described in Materials and methods. **(a)** HUVECs were cultured in chamber slides on CM for 24 h and incubated with anti-uPAR antibody followed by Alexa Fluor-488-conjugated secondary antibody at 4 °C. Cells were again labeled with Alexa Fluor-595-CtXb subunit. Slides were mounted and analyzed by confocal microscopy. Negative controls, using an isotype antibody, showed no staining (inset). Serum-free medium (SFM) and DDK-tag containing rh-uPAR were used as controls. To disrupt lipid rafts, HUVECs were pretreated with MBCD, as described in Materials and methods. **(b)** HUVECs lipid rafts were isolated as described in Materials and methods. Lipid raft-enriched fractions were analyzed for uPAR and DDK-tag levels using immunoblot analysis. Flotillin-1 and caveolin-1 served as controls. Protein band intensities were quantified by densitometric analysis using ImageJ software (NIH). The levels of uPAR protein were normalized to protein levels in HUVECs cultured on parental-CM. Columns: mean; bars: s.d.; $n = 3$; * $P < 0.01$ vs parental-CM. **(c)** Invasion and migration assays were performed as described in Figure 1d *In vitro* angiogenesis assay was performed as described in Figure 1. To deplete cholesterol, HUVECs were pretreated with MBCD as described in Materials and methods (**c** and **d**). Columns: mean; bars: s.d.; $n = 3$; * $p < 0.01$ vs parental-CM; ** $p < 0.01$ vs UR-CM.

Tumor-associated s-uPAR induces ERK/Rac1-mediated migration and tube formation in HUVECs

A recent study on uPAR-integrin pathways demonstrated that ERK mediated activation of Rac1,²⁸ which is an important event in promotion of uPAR-mediated cell motility, invasion and angiogenesis.^{29,30} To investigate whether tumor-associated s-uPAR enhances phosphorylation of ERK1/2 and activation of Rac1, we performed immunoblot analyses for phospho-ERK1/2 and pull-down assay for active Rac1 using HUVEC lysates. Tumor-associated s-uPAR induced phosphorylation of ERK1/2 and activation of Rac1 in HUVECs cultured on UR-CM compared with cells cultured on EV-CM. In contrast, phospho-ERK1/2 and activate-Rac1 were significantly decreased in HUVECs cultured on UR-Si-CM as compared with cells cultured on EV-CM (Figures 4a and b). Similarly, supplementation of rh-uPAR also induced ERK1/2 phosphorylation and Rac1 activation (Figures 4a and b).

Further, functional blocking uPAR-Ab, pharmacological inhibitor for ERK (U0126) or expression of dominant-negative mutant of Rac1 (Dn-Rac1) mitigated UR-CM-induced ERK1/2 phosphorylation and Rac1 activity (Figures 4c and e). In addition, uPAR-Ab, U0126 or Dn-Rac1 expression diminished s-uPAR-induced HUVEC migration and invasion *in vitro* (Figure 4f).

Full-length s-uPAR recruits on HUVEC membrane *in vitro*

As s-uPAR exists in three forms, that is, full-length s-uPAR (D1-D3; 37 kDa), truncated s-uPAR (D2-D3; ~27 kDa) and truncated s-uPAR containing N-terminal domain (D1; ~16 kDa),³¹ we analyzed CM

by immunoblotting after deglycosylation of CM. We observed two s-uPAR forms corresponding to full-length and truncated D2-D3, in an approximately equimolar ratio (Figure 5a and Supplementary Figure S3). Further, deglycosylation followed by immunoblot analysis of the membrane fraction of HUVECs cultured on UR-CM demonstrated that higher amounts of full-length s-uPAR recruited onto the HUVEC membrane (Figure 5b), suggesting that full-length s-uPAR from tumor cells recruits onto the HUVEC membrane and involves in induction of cell migration.

uPAR overexpression enhances *in vivo* angiogenesis

We examined whether overexpression of uPAR could elicit tumor angiogenesis *in vivo* as assessed by the dorsal air sac model.²⁴ Implantation of a chamber containing 4910UR cells or rh-uPAR in the dorsal air sac resulted in the development of microvessels with curved thin structures and many tiny bleeding spots as compared with 4910EV cells. In contrast, implantation of 4910UR-Si cells resulted in the development of only a few additional microvessels (Figure 5c).

uPAR overexpression enhances circulating s-uPAR levels *in vivo*

We next sought to determine whether circulation of s-uPAR correlates with tumor angiogenesis and tumor growth in an orthotopic tumor model.^{8,21,32} Circulation of s-uPAR in blood on day 15 after cell implantation was 0.9–1.1 ng/ml and increased drastically to 1.7–3.7 ng/ml by day 40 in controls. In contrast, circulation of s-uPAR in blood drastically increased from 3.2–4.2 ng/ml on day 15 to 20–25 ng/ml on day 40 as tumor burden

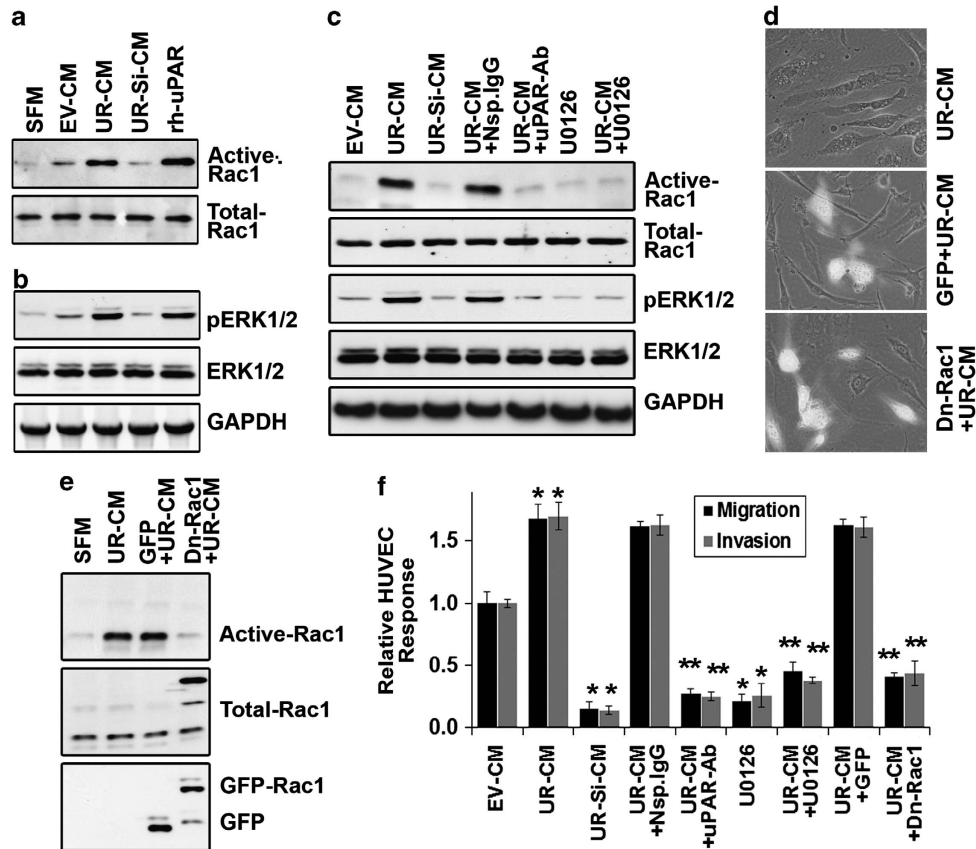


Figure 4. s-uPAR induces ERK/Rac1-mediated migration and tube formation in HUVECs. Conditioned medium (CM) was collected from tumor cells, as described in Materials and methods. (a) HUVECs lysates were used to perform GST-Rac1 pull-down assay. The protein complexes were subjected to immunoblot analysis to detect active Rac1. Rac1 from total cell lysates was used as a control. (b) Total cell lysates were subjected to immunoblot analysis for phospho-ERK1/2 (pERK1/2) and total ERK1/2. Glyceraldehyde 3-phosphate dehydrogenase (GAPDH) served as a loading control. HUVECs grown on rh-uPAR were used as a control. (c) HUVECs were cultured on CM alone and/or supplemented with functional blocking anti-uPAR antibody (uPAR-Ab) or isotype control (Nsp.IgG.) or MEK inhibitor (U0126) for 24 h. Cell lysates or GST-Rac1 pull-down protein complexes were subjected to immunoblot analysis to detect active Rac1, Rac1 pERK1/2 and ERK1/2. GAPDH served as a loading control. (d) HUVECs were transfected with dominant-negative mutant Rac1 (Dn-Rac1) for 24 h and cultured on UR-CM. Micrographs were captured for green fluorescent protein (GFP) expression (green) and phase contrast (gray) immediately after the addition of UR-CM (magnification $\times 60$). (e) HUVECs were transfected with Dn-Rac1 for 24 h, cultured on CM for another 24 h, collected and lysed. GST-Rac1 pull-down protein complexes were subjected to immunoblot analysis to detect active Rac1. GFP and Rac1 from total cell lysates were used as controls. (f) HUVECs were transfected with Dn-Rac1 for 24 h and cultured on CM alone and/or supplemented with uPAR-Ab, or Nsp.IgG or U0126 for another 24 h. Invasion and migration assays were performed as described in Figure 1. Columns: mean; bars: s.d.; $n = 3$; * $P < 0.01$ vs parental-CM; ** $P < 0.01$ vs UR-CM.

increased in mice bearing tumors of UR cells (Figures 5d and e). However, blood serum s-uPAR levels were remarkably low (0.015–0.020 ng/ml) in mice bearing tumors of UR-Si cells (Figures 5d and e). Further, deglycosylation of serum samples indicated that full-length forms of s-uPAR were more predominant than truncated D2-D3 and D3 forms in mice blood (Figure 5f).

uPAR overexpression enhances tumor growth and vascularity *in vivo*

Histological analysis of hematoxylin and eosin-stained tumor sections demonstrated that UR cells had higher tumor volume (> 2 – 2.5 -fold) compared with EV cells. Notably, UR-Si cells showed growth delay by 75–80% ($P < 0.01$) compared with EV tumors in mice (Figures 6a and b). Further, the tumor cores of the EV, UR and UR-Si xenografts from mice were analyzed immunohistologically with anti-uPAR, anti-vascular endothelial growth factor anti-tomato lectin. Immunoreactivity of vascular endothelial growth factor and tomato lectin in the tissue sections from the tumors derived from mice from each group provided some measure of vascularity as affected by uPAR suppression (Figure 6c). Compared with EV tumors, sections from UR-Si tumors showed decreased

immunoreactivity of tomato lectin and vascular endothelial growth factor. To confirm uPAR recruiting on endothelial cell membrane, we performed double staining immunofluorescent studies for anti-DDK-tag with either anti-von Willebrand factor or anti-CD31 on UR tumor sections. Figures 6d and e show colocalization of von Willebrand factor and DDK, indicating that uPAR from tumor cells recruited onto endothelial cells, and therefore might be involved in endothelial migration and angiogenesis.

DISCUSSION

The uPA/uPAR system has a critical role in tumor vascular biology by facilitating cell migration and modulating angiogenesis.^{8,32} The presence of uPAR on endothelial cells and its functional significance in migration have been described previously.^{8,10,26} However, to our knowledge, the consequences of paracrine signaling of uPAR have not been investigated. The present study is the first demonstration that illustrates the intricacies involved in the regulation of tumor-associated s-uPAR in connection with migration and angiogenesis. Here, we demonstrate tumor-associated s-uPAR recruitment onto endothelial membrane

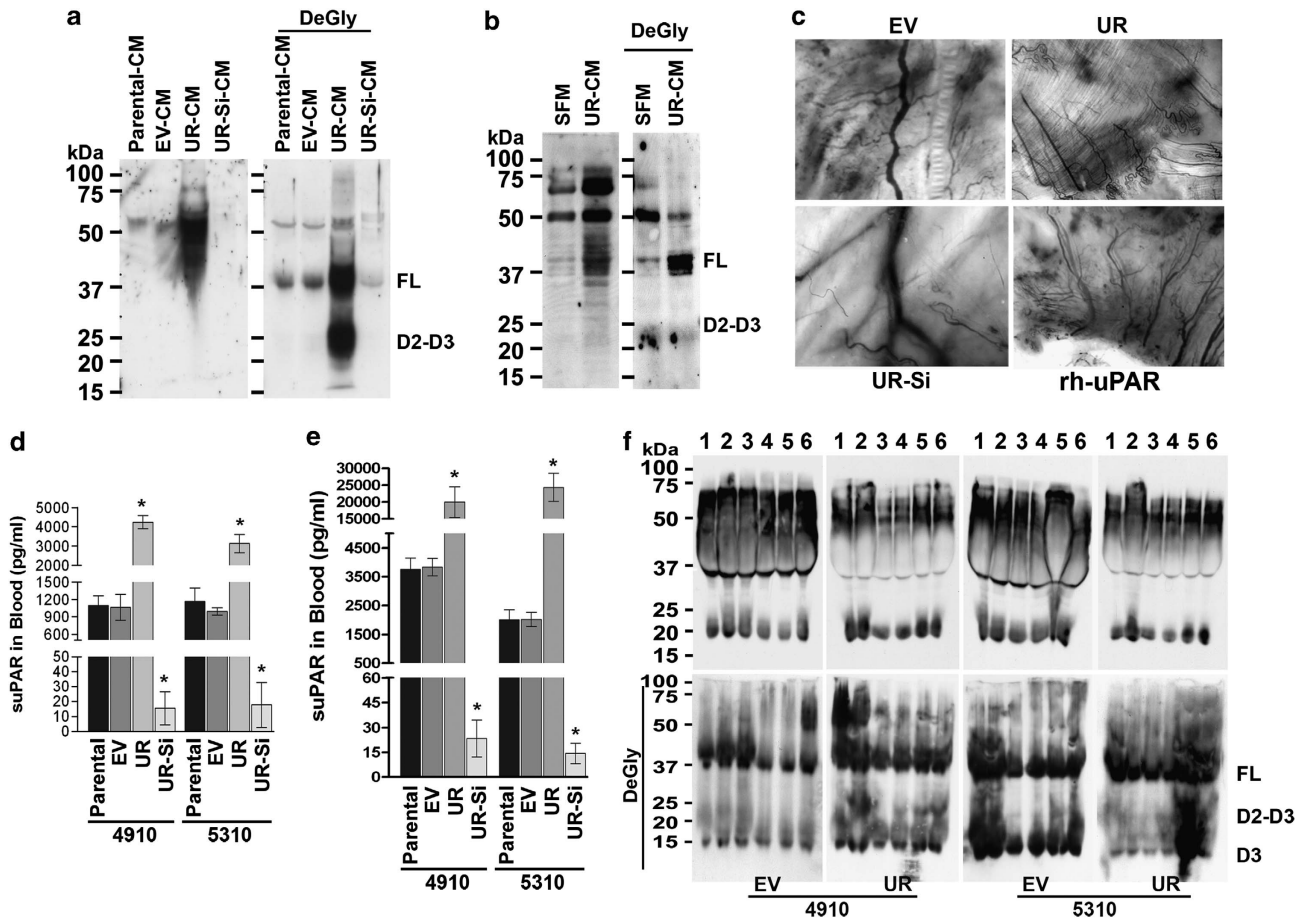


Figure 5. Diverse forms of tumor-associated s-uPAR *in vitro* and *in vivo*. **(a)** Conditioned medium (CM) was collected from tumor cells as described in Materials and methods. CM was subjected to deglycosylation using a deglycosylation kit and analyzed by immunoblot for uPAR using specific antibodies. **(b)** Equal amount of proteins containing HUVEC lysates were used for extraction of cell membrane fractions and were subjected to deglycosylation, and analyzed by immunoblot for uPAR using specific antibodies. **(c)** *In vivo* angiogenic assay was performed by using the dorsal air sac model. 4910EV (EV), 4910UR (UR), 4910UR-Si (UR-Si) cells or a recombinant human uPAR (rh-uPAR) containing chamber was implanted in the dorsal cavity of mice. The micrographs for the presence of tumor-induced neovasculature (microvessels with curved thin structures and many tiny bleeding spots) and pre-existing vasculature (straight) were captured. Representative micrographs are shown. **(d, e)** Blood was collected from mice orthotopically xenografted with stably expressing EV, UR and UR-Si cells. Total uPAR levels were estimated using a commercial human uPAR Quantikine Immunoassay kit according to the manufacturer's instructions. The data quantification for a set I ($n=4$; **d**) and set II ($n=6$; **e**), on day 15 and 40, respectively, after cell implantation are shown. Columns: mean; bars: s.d.; * $P<0.01$ vs parental control. **(f)** Blood serum (from mice 1–6; on day 40) was subjected to deglycosylation and analyzed by immunoblot for uPAR using specific antibodies. D2-D3, D2-D3 domain containing truncated s-uPAR; D3, D3 domain containing truncated s-uPAR; FL, full-length s-uPAR; .

cholesterol-rich microdomains known as lipid rafts of endothelial cells and stimulation of ERK1/2- and Rac1-mediated migration, and subsequently, angiogenesis. Further, uPAR knockdown drastically reduced circulating s-uPAR levels in mice blood serum, as well as endothelial cell recruitment and vasculature in orthotopic xenograft tumors *in vivo*.

The overexpression of uPAR in various cancers has been demonstrated in many studies.^{5,14–17} Of note, s-uPAR has been found in the biological fluids of cancer patients and is highly correlated with tumor malignancy.^{17–19} Enhanced serum s-uPAR concentrations have been tied to poor prognosis in a variety of cancer patients, and as such, may have prognostic value in a large number of human cancers.^{33–36} In this study, we present evidence demonstrating a significant positive association between tumor angiogenesis and s-uPAR, suggesting a plausible connection with tumor vasculature. Here, we used 4910 and 5310 xenograft cells with stable expression of myc-DDK-tagged open reading frame clone of human uPAR to generate s-uPAR and for *in vivo* studies. We measured s-uPAR released into CM during the growth of the tumor cells (EV, UR and UR-Si) *in vitro* and *in vivo*. Our study shows

that the levels of s-uPAR in the plasma of host mice during the growth of xenografted cells were highly correlated with tumor volume. Our *in vitro* studies demonstrated tumor-associated s-uPAR recruitment onto HUVEC membrane and the ability to induce cell motility. HUVECs cultured on UR-CM showed a significant increase in uPAR levels in the cell membrane fraction as compared with controls. However, the membrane fraction from HUVECs cultured on UR-Si-CM did not exert a significant effect on uPAR levels. As uPAR is anchored to the cell membrane through a glycosylphosphatidylinositol tail, which accounts for its presence in lipid rafts,^{6,7,21,37} and orchestrates the signaling pathways underlying the functional changes,³⁸ we analyzed the lipid raft fractions for s-uPAR recruitment onto membrane rafts. Here, we show evidence of tumor-associated s-uPAR accumulation in HUVECs' lipid rafts. However, cells grown on UR-Si-CM did not show any significant accumulation of s-uPAR onto membrane rafts, whereas supplementation of rh-uPAR-DDK showed a significant colocalization of uPAR and GM1 in lipid rafts. Next, we disrupted the integrity of the lipid raft, which is essential in many cellular functions including angiogenesis^{8,10,26} using a

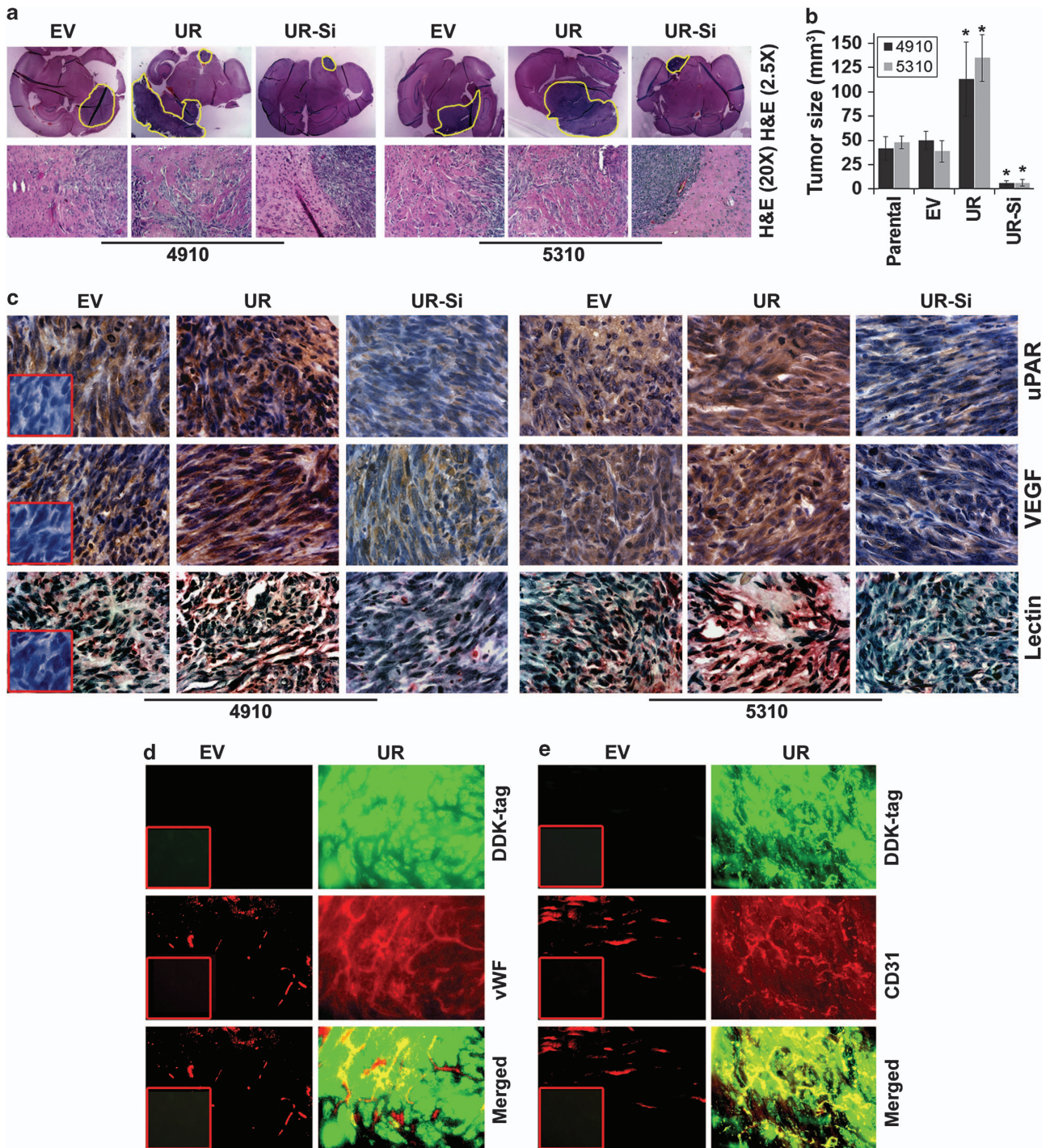


Figure 6. uPAR overexpression enhances tumor growth, vascularity and s-uPAR recruits onto endothelial cells *in vivo*. **(a)** Stably expressing EV, UR and UR-Si cells were injected intracerebrally into mice. Mice were euthanized and brains were collected and fixed as described in Materials and methods. Brain sections were stained with hematoxylin and eosin (H&E) solution, and representative micrographs are shown (upper panel). H&E-stained micrographs showing the tumor invasive front ($\times 20$; lower panel). **(b)** Brain tumor areas were calculated using Image Pro Discovery Program software (Media Cybernetics, Inc., Rockville, MD, USA). Columns: mean; bars: s.d.; $n=6$; $*P<0.01$ vs parental controls. **(c)** Immunohistochemical analysis of brain sections using anti-uPAR and anti-vascular endothelial growth factor (VEGF). Blood vessels in tumor sections were visualized with biotin-labeled tomato lectin. Inset: isotype control. **(d, e)** Fluorescence microscopy for colocalization of an endothelial cell marker (von Willebrand factor (vWF)/anti-CD31) and DDK-tag in tumor sections from mice that were implanted with 4910 EV (EV) and 4910UR (UR) cells. Inset, isotype control.

known cholesterol disrupting agent, MBCD. We observed that the treatment of cells with MBCD impaired invasion, migration and capillary morphogenesis, thus demonstrating that the tumor-associated s-uPAR recruits onto HUVECs membrane and induces cell migration and angiogenesis.

s-uPAR exists in the forms of full-length (D1-D3), truncated (D2-D3) and truncated containing N-terminal domain (D1), which show different properties owing to structural differences.³¹ Studies on full-length s-uPAR demonstrated that it can act as an uPA scavenger and inhibit cancer cell growth and invasion in a

variety of cancers.^{39–41} Full-length s-uPAR contains intact domains that are able to compete with cellular full-length uPAR for uPA and is able to bind both uPA and vitronectin. Hence, s-uPAR can affect the processes catalyzed by those molecules and their interaction with membrane-bound uPAR.^{39–41} In contrast, the cleaved D2-D3 forms with SRSRY (residues 88–92) sequence in the linker region has been shown to be a chemotactic agent.^{31,42,43} However, in the present study, the deglycosylation and immunoblot analyses revealed that two s-uPAR forms corresponding to full-length and truncated D2-D3 were present in CM samples in an approximately equimolar ratio. Further, deglycosylation of the membrane fraction and membrane raft fraction of HUVECs cultured on UR-CM demonstrated that higher amounts of full-length s-uPAR forms (vs truncated) were recruited onto cell membrane. Therefore, we speculate full-length s-uPAR present in the matrix milieu acts as an uPA scavenger, and once it recruits onto the endothelial cell membrane it is able to induce endothelial cell migration.

Cellular uPAR is distributed on the cell surface at focal contacts initially, and will localize into aggregates on the leading edge of migrating cells^{18,43,44} and is believed to regulate the activation state of integrins by altering their adhesive properties as well as signaling capacity.^{45–47} A large body of evidence demonstrates integrin-mediated uPAR signaling associated with the activation of FAK and ERK,²⁶ and downstream Rho family small GTPase Rac1.²⁸ A recent study shows that uPAR-/integrin-mediated activation of ERK is necessary for the subsequent activation of Rac1.²⁸ Activation of Rac1 has emerged as an important event in the promotion of motility and invasion by uPAR.^{29,30} Ectopic uPAR expression results in Rac1-dependent lamellipodial protrusion and cell motility,^{29,40} and inhibiting endogenous uPAR expression inactivates Rac1 and strongly inhibits lamellipodial protrusion and cell motility.^{30,48} In the present study, EV-CM induced significant levels of HUVEC migration, whereas UR-CM augmented HUVEC migration levels remarkably. In contrast, UR-Si-CM or functional blocking uPAR-Ab inhibited s-uPAR-mediated migration and angiogenesis. Interestingly, supplementation of rh-uPAR alone enhanced HUVEC migration and capillary tube formation significantly. In addition, supplementation of rh-uPAR resumed UR-Si-CM-inhibited cell migration and capillary tube formation. Further, phosphorylation of ERK1/2 and activation of Rac1 were significantly elevated in HUVECs cultured on UR-CM compared with cells cultured on EV-CM. In contrast, phosphorylation of ERK1/2 and activation of Rac1 were inhibited remarkably in HUVECs cultured on UR-Si-CM as compared with cells cultured on EV-CM. Notably, supplementation of rh-uPAR induced phosphorylation of ERK and activity of Rac1 similar to s-uPAR-containing UR-CM. Further, uPAR-Ab, Dn-Rac1 and U0126 mitigated UR-CM-induced HUVEC migration and invasion *in vitro*. A recent study on uPAR demonstrated that endothelial progenitor cell-dependent angiogenesis requires localization of the full-length form of uPAR in lipid rafts.⁸ Our results showed that the deglycosylation of lipid raft fractions of HUVECs grown on UR-CM have significant amounts of full-length s-uPAR residing onto membrane. Further, *in vivo* dorsal air sac model experiments demonstrated that implantation of uPAR-overexpressed cells induced profound neovascularization as compared with control cells. Further, implantation of rh-uPAR alone also induced significant high levels of neovascularization *in vivo*. In contrast, UR-Si cells failed to induce significant neovascularization in mice, thereby suggesting s-uPAR involvement in angiogenesis.

Our *in vivo* experiments demonstrated that s-uPAR levels in blood serum of mice that were bearing tumors of uPAR-overexpressed cells showed high levels (20–25 ng/ml) as compared with mice that were bearing tumors of EV cells (3.2–4.2 ng/ml). Conversely, a drastic reduction of s-uPAR levels was observed in blood serum of mice that were bearing tumors of UR-Si cells (0.015–0.020 ng/ml) as compared with mice that were bearing tumors of EV cells (3.2–4.2 ng/ml). Immunoblot analysis of

deglycosylated blood serum samples from mice that were bearing tumors of UR cells exhibited full-length and D2-D3 forms of s-uPAR, which was similar to *in vitro* cells. Further, a highly significant correlation was found between tumor volume and plasma s-uPAR concentration in xenografted mice, thereby indicating that plasma levels of s-uPAR reflect tumor burden in the host mice. Further, immunoreactivity of vascular endothelial growth factor and tomato lectin, and colocalization of DDK with either von Willebrand factor or CD31 in tumor sections showed a positive correlation with circulating s-uPAR levels and tumor burden in mice, thereby suggesting s-uPAR involvement in angiogenesis.

In conclusion, determination of the molecular mechanisms underlying s-uPAR paracrine signaling, such as the Rac1 activation-mediated pathway described here, is essential to provide insight into the well-established role of uPAR in tumor progression. Understanding these pathways will provide new therapeutic targets for the prevention of human tumor metastasis, angiogenesis and growth.

MATERIALS AND METHODS

Cell culture

The xenograft cell lines 4910 and 5310 (kindly provided by Dr David James, University of California at San Francisco) were generated and maintained in mice, and are highly invasive in the mouse brain.⁴⁹ At 3–4 passages of cells from mice heterotopic tumors were frozen and these stocks were used for further experiments up to 10 passages to obtain consistent results. Cells were cultured in Roswell Park Memorial Institute medium-1640 (Mediatech Inc., Manassas, VA, USA) medium, as described previously.²¹ Cells were authenticated on the basis of amplification of *EGFR* and *PDGFR α* , homozygous deletion of *CDKN2A*, and mutation of *PTEN* and *p53* by the provider.⁴⁹ HUVECs were obtained from Lonza (Walkersville, MD, USA) and maintained using the EGM-2 bullet kit. HUVECs were authenticated by expression of CD31/105, von Willebrand Factor and uptake of acetylated low-density lipoprotein. All experiments were conducted on vitronectin-coated dishes unless otherwise mentioned. Cells were incubated at 37 °C in a humidified 5% CO₂ atmosphere.

Antibodies and reagents

We used the following antibodies, reagents and kits in this study: anti-uPAR (10G7), anti-uPAR (FL-290), anti-uPAR (N-19), anti-uPAR (IID7), anti-uPAR (IIIF10), anti-transferrin receptor, anti- α -tubulin, anti-flotillin-1, anti-flotillin-2, anti-ERK1/2, anti-phospho-ERK1/2, anti-glyceraldehyde 3-phosphate dehydrogenase, secondary antibodies (horseradish peroxidase-, Alexa Fluor-conjugated, Santa Cruz Biotechnology, Santa Cruz, CA, USA), isotype control antibodies (Santa Cruz Biotechnology), anti-Rac1, anti-DDK-tag, (Cell Signaling Technology, Beverly, MA, USA), Biotinylated Tomato Lectin, Vectastain ABC-AP, Vector Red Alkaline Phosphatase Substrate Kit (Vector Laboratories, Burlingame, CA, USA), Growth Factor Reduced Matrigel (BD Biosciences, San Jose, CA, USA), rh-uPAR with DDK-tag (rh-uPAR), uPAR Quantikine Immunoassay kit, functional blocking anti-uPAR-Ab (R&D Systems, Minneapolis, MN, USA), MEK inhibitor U0126 (Promega Corporation, Madison, WI, USA), Mem-PER Eukaryotic Membrane Protein Extraction Kit (Thermo Scientific, Dubuque, IA, USA), Enzymatic Protein Deglycosylation Kit, MBCD and Caveolae/Raft isolation kit (Sigma, St Louis, MO, USA).

Plasmid transfections and other treatments

The siRNA constructs for uPAR and a control siRNA with pcDAN3.1 (Invitrogen, San Diego, CA, USA) back bone were prepared as described previously.²¹ siRNA constructs against uPAR and Myc-DDK-tagged open reading frame clone of uPAR (puPAR-FL), transcript variant-1 were purchased from OriGene (Rockville, MD, USA). pGEX-Rac1 (#12200) and Dn-Rac1 (pcDNA-EGFP-Rac1-T17N; Dn-Rac1; #12982) plasmids were obtained from Addgene Inc. (Cambridge, MA, USA). For all transient or stable transfections, FuGeneHD transfection reagent (Roche, Indianapolis, IN, USA) was used. The 4910/5310 cells were transfected with EV (#12200), puPAR-FL or puPAR-Si, and stably expressing uPAR-FL (UR), UR-Si or vector control (EV) cell lines were generated by selecting with G418 and/or puromycin.

Where detailed, cell invasion, migration, angiogenesis and other experiments were performed in the presence of functional blocking

anti-uPAR-Ab or isotype control antibody (10 µg/ml), or rh-uPAR (100 µg/ml) or after Dn-Rac1 transfection. In other experiments, HUVECs were pretreated with MBCD (2.5 mg/ml) for 30 min for depletion of cholesterol.

Preparation of CM

The medium was removed from cells after 24 h of either transient transfection or plating, and 3 ml of serum-free medium was added followed by incubation overnight. Tumor-CM was collected and used for either culturing of HUVECs or immunoblotting experiments. Experiments were performed in the presence of endothelial basal medium as control, as required.

Immunoblotting

Cells were lysed in a buffer containing 1% Triton-X-100, 150 mM NaCl and 50 mM Tris (pH 7.5).²¹ For extraction of cell membrane fractions, we used Mem-PER Eukaryotic Membrane Protein Extraction Kit as per the manufacturer's instructions. Equal amounts of protein fractions were used for immunoblot analysis, as described previously.²¹ Comparable loading of proteins on the gel was verified by reprobing the blots with an antibody specific for *GAPDH*.

Migration and invasion assays

Tumor cell-induced HUVEC migration was measured using the two-chambered culture inserts (ibidi, Verona, WI, USA). The culture inserts were placed onto eight-well chamber slides and seeded Qtracker dyes (Life Technologies, Grand Island, NY, USA)-labeled tumor cells and HUVECs into separate chambers (1×10^4 cells per chamber). Cells were cultured for 16 h and the culture inserts were removed to create cell-free gaps between attached cells. In other experiments both chambers were seeded with unlabeled HUVECs and cultured on CM. Cells were allowed to migrate for a further 24 h. Images were captured at 0 and 24 h of incubation.

Tumor cell-induced HUVEC invasion was studied in ThinCert™ inserts with 8 µm porous filters (Greiner Bio-One, Monroe, NC, USA) coated with vitronectin containing Matrigel. HUVECs (2×10^5) were seeded on the top of the membrane while CM from tumor cells was added to the lower chamber. After 16 h incubation, filters were washed, fixed and stained. The migrated cells on the reverse side of the membrane were photographed and expressed as the absolute number of migrated cells.

In vitro tube formation and *in vivo* angiogenesis assays

In vitro tube formation assay was performed as described earlier.²⁴ HUVECs (2×10^4) were grown in the presence of CM or serum-free medium in 96-well plates precoated with Matrigel. After 24 h incubation, photographs were taken and the degree of tube formation was quantified by measuring the cumulative tube length using ImageJ software (NIH, Bethesda, MD, USA).

Angiogenic response *in vivo* was examined with the dorsal air sac assay by implanting diffusion chambers with stably expressing 4910EV, 4910UR and 4910UR-Si cells (2×10^5), and rh-uPAR in serum-free medium were placed underneath the skin into the superficial incision, as described previously.²⁴ The number of blood vessels within the chamber in the area of the air sac fascia was counted and quantified.

Flow cytometry

HUVECs were cultured on CM for 24 h and labeled with anti-uPAR-Ab for 1 h, followed by Alexa Fluor-488-conjugated secondary antibody for 30 min before samples were analyzed on a FACS Calibur Flow Cytometer (BD Biosciences). Data acquisition and analysis were performed using CellQuest software (BD Biosciences).

Lipid raft isolation

Lipid rafts were isolated from cells using a caveolae/rafts isolation kit (Sigma) as described earlier.²¹ Briefly, 24 h after culture of HUVECs on CM, cells were labeled with CTxB (β subunit of the cholera toxin)-horseradish peroxidase and lysed in Triton-X-100 buffer, and then fractionated by gradient centrifugation (22 h; 40000 r.p.m. at 4 °C). Ten fractions were collected from the top of the gradient. Raft and non-raft fractions were determined by dot blot analysis, and positive fractions for GM1 (fractions 2–4) were pooled. The purity of raft and non-raft fractions was confirmed by immunoblot analysis using specific antibodies against raft- and non-raft-associated markers.

Enzyme-linked immunosorbent assay

Blood plasma or CM was prepared as mentioned in appropriate sections, and s-uPAR levels were determined using a commercial human uPAR Quantikine Immunoassay kit (R&D Systems) according to the manufacturer's instructions.

Deglycosylation

Equal quantities of HUVEC membrane fractions, blood serum and CM were deglycosylated using a deglycosylation kit (New England Biolabs, Ipswich, MA, USA) as per the manufacturer's instructions. Deglycosylated proteins were subjected to immunoblot analysis using different anti-uPAR-Ab.

Immunofluorescent and immunohistochemical analyses

Immunofluorescent and immunohistochemical analyses were performed as described.²¹ Deparaffinized and rehydrated tissue sections or fixed cells were blocked by goat serum followed by incubation with primary antibodies. Isotype control antibody was used as a negative control. Expression was detected with either Alexa Fluor-conjugated secondary antibody or horseradish peroxidase-conjugated secondary antibody, followed by 3,3'-diaminobenzidine solution. The nucleus was counterstained with either 4',6'-diamidino-2-phenylindole or hematoxylin, and photographed. For lipid raft labeling,^{21,25} HUVECs were incubated with anti-DDK antibody followed by Alexa Fluor-488-conjugated secondary antibody. Next, samples were labeled with Alexa Fluor-595-CTxB subunit as a raft marker. Slides were mounted and analyzed using a confocal microscope. To disrupt lipid rafts, HUVECs were pretreated with MBCD (2.5 mg/ml) for 30 min, and cells were incubated for 24 h on CM.

Measurement of Rac1 activity

The GST-Rac1 (p21-binding domain of Pak1 fused to glutathione-S-transferase) pull-down assays were used to detect cellular activated (GTP-bound) Rac1, as described previously.⁵⁰ Briefly, HUVEC lysates were incubated with GST-Rac1-coupled glutathione sepharose beads. The beads were washed extensively, and proteins bound on beads were examined by immunoblot analysis with anti-Rac1 antibody.

Orthotopic animal models

Stable expressing EV, UR or UR-Si cells (2×10^5) were injected intracerebrally into athymic nude mice (10 per group), as described previously.²¹ At the time of killing, blood was collected from deeply anesthetized mice (four on day 15 and six on day 40 after cells implantation) by cardiac puncture and rapidly mixed with cold trisodiumcitrate (0.1 vol) to give a final concentration of 12.9 mM citrate. The plasma was separated from blood cells within 1 h by centrifugation at 2000 g for 30 min at 4 °C, and the supernatant was stored at –80 °C before assay. The brains collected from these mice were fixed in 10% buffered formaldehyde. To visualize tumor cells, the brain sections (5 µm) were stained with hematoxylin and eosin and the tumor volume was quantified as described previously.²²

Statistical analysis

All data are presented as mean ± s.d. of at least three independent experiments. ImageJ software (NIH) was used for quantification of migration, angiogenesis and band intensities of mRNA and protein gels. Results were analyzed using a two-tailed Student's *t*-test to assess statistical significance. Statistical significances were accepted at $P < 0.05$ and $P < 0.01$.

CONFLICT OF INTEREST

The authors declare no conflict of interest.

ACKNOWLEDGEMENTS

We thank Diana Meister and Sushma Jasti for manuscript review. We also thank Dr David James (University of California at San Francisco, CA) for providing 4910 and 5310 cells. This research was supported by a grant from the National Institute of Neurological Disorder and Stroke (NS047699 to JSR).

DISCLAIMER

The contents of this manuscript are solely the responsibility of the authors and do not necessarily represent the official views of the National Institutes of Health.

REFERENCES

- Folkman J. Angiogenesis: an organizing principle for drug discovery? *Nat Rev Drug Discov* 2007; **6**: 273–286.
- Bergers G, Benjamin LE. Tumorigenesis and the angiogenic switch. *Nat Rev Cancer* 2003; **3**: 401–410.
- Lamalace L, Le BF, Huot J. Endothelial cell migration during angiogenesis. *Circ Res* 2007; **100**: 782–794.
- Ossowski L. Effect of antisense inhibition of Urokinase receptor on malignancy. *Curr Top Microbiol Immunol* 1996; **213**: 101–112.
- Bajou K, Noel A, Gerard RD, Masson V, Brunner N, Holst-Hansen C et al. Absence of host plasminogen activator inhibitor 1 prevents cancer invasion and vascularization. *Nat Med* 1998; **4**: 923–928.
- Patra SK. Dissecting lipid raft facilitated cell signaling pathways in cancer. *Biochim Biophys Acta* 2008; **1785**: 182–206.
- Kiyan J, Smith G, Haller H, Dumler I. Urokinase-receptor-mediated phenotypic changes in vascular smooth muscle cells require the involvement of membrane rafts. *Biochem J* 2009; **423**: 343–351.
- Margheri F, Chilla A, Laurenzana A, Serrati S, Mazzanti B, Saccardi R et al. Endothelial progenitor cell-dependent angiogenesis requires localization of the full-length form of uPAR in caveolae. *Blood* 2011; **118**: 3743–3755.
- Carlin SM, Resink TJ, Tamm M, Roth M. Urokinase signal transduction and its role in cell migration. *FASEB J* 2005; **19**: 195–202.
- Prager GW, Breuss JM, Steurer S, Olcaydu D, Mihaly J, Brunner PM et al. Vascular endothelial growth factor receptor-2-induced initial endothelial cell migration depends on the presence of the urokinase receptor. *Circ Res* 2004; **94**: 1562–1570.
- Lu H, Mabilat C, Yeh P, Guittou JD, Li H, Pouchalet M et al. Blockage of urokinase receptor reduces in vitro the motility and the deformability of endothelial cells. *FEBS Lett* 1996; **380**: 21–24.
- Fibbi G, Caldini R, Chevanne M, Pucci M, Schiavone N, Morbidelli L et al. Urokinase-dependent angiogenesis in vitro and diacylglycerol production are blocked by antisense oligonucleotides against the urokinase receptor. *Lab Invest* 1998; **78**: 1109–1119.
- Raghu H, Lakka SS, Gondi CS, Mohanam S, Dinh DH, Gujrati M et al. Suppression of uPA and uPAR attenuates angiogenesis mediated angiogenesis in endothelial and glioblastoma cell lines. *PLoS One* 2010; **5**: e12458.
- Kennedy S, Duffy MJ, Duggan C, Barnes C, Rafferty R, Kramer MD. Semi-quantitation of urokinase plasminogen activator and its receptor in breast carcinomas by immunocytochemistry. *Br J Cancer* 1998; **77**: 1638–1641.
- Werle B, Kotsch M, Lah TT, Kos J, Gabrijelcic-Geiger D, Spiess E et al. Cathepsin B, plasminogenactivator-inhibitor (PAI-1) and plasminogenactivator-receptor (uPAR) are prognostic factors for patients with non-small cell lung cancer. *Anticancer Res* 2004; **24**: 4147–4161.
- Salajegheh M, Rudnicki A, Smith TW. Expression of urokinase-type plasminogen activator receptor (uPAR) in primary central nervous system neoplasms. *Appl Immunohistochem Mol Morphol* 2005; **13**: 184–189.
- Rasch MG, Lund IK, Almasi CE, Hoyer-Hansen G. Intact and cleaved uPAR forms: diagnostic and prognostic value in cancer. *Front Biosci* 2008; **13**: 6752–6762.
- de Bock CE, Wang Y. Clinical significance of urokinase-type plasminogen activator receptor (uPAR) expression in cancer. *Med Res Rev* 2004; **24**: 13–39.
- Hoyer-Hansen G, Lund IK. Urokinase receptor variants in tissue and body fluids. *Adv Clin Chem* 2007; **44**: 65–102.
- Kunigal S, Lakka SS, Gondi CS, Estes N, Rao JS. RNAi-mediated downregulation of urokinase plasminogen activator receptor and matrix metalloproteinase-9 in human breast cancer cells results in decreased tumor invasion, angiogenesis and growth. *Int J Cancer* 2007; **121**: 2307–2316.
- Chetty C, Lakka SS, Bhoopathi P, Gondi CS, Veeravalli KK, Fassett D et al. Urokinase plasminogen activator receptor and/or matrix metalloproteinase-9 inhibition induces apoptosis signaling through lipid rafts in glioblastoma xenograft cells. *Mol Cancer Ther* 2010; **9**: 2605–2617.
- Badiga AV, Chetty C, Kesanakurti D et al. MMP-2 siRNA inhibits radiation-enhanced invasiveness in glioma cells. *PLoS One* 2011; **6**: e20614.
- Gorantla B, Asuthkar S, Rao JS, Patel J, Gondi CS. Suppression of the uPAR-uPA system retards angiogenesis, invasion, and in vivo tumor development in pancreatic cancer cells. *Mol Cancer Res* 2011; **9**: 377–389.
- Chetty C, Lakka SS, Bhoopathi P, Kunigal S, Geiss R, Rao JS. Tissue inhibitor of metalloproteinase 3 suppresses tumor angiogenesis in matrix metalloproteinase 2-down-regulated lung cancer. *Cancer Res* 2008; **68**: 4736–4745.
- Gajate C, Mollinedo F. The antitumor ether lipid ET-18-OCH(3) induces apoptosis through translocation and capping of Fas/CD95 into membrane rafts in human leukemic cells. *Blood* 2001; **98**: 3860–3863.
- Liu D, Aguirre GJ, Estrada Y, Ossowski L. EGFR is a transducer of the urokinase receptor initiated signal that is required for in vivo growth of a human carcinoma. *Cancer Cell* 2002; **1**: 445–457.
- Simons K, Toomre D. Lipid rafts and signal transduction. *Nat Rev Mol Cell Biol* 2000; **1**: 31–39.
- Smith HW, Marra P, Marshall CJ. uPAR promotes formation of the p130Cas-Crk complex to activate Rac through DOCK180. *J Cell Biol* 2008; **182**: 777–790.
- Kjoller L, Hall A. Rac mediates cytoskeletal rearrangements and increased cell motility induced by urokinase-type plasminogen activator receptor binding to vitronectin. *J Cell Biol* 2001; **152**: 1145–1157.
- Vial E, Sahai E, Marshall CJ. ERK-MAPK signaling coordinately regulates activity of Rac1 and RhoA for tumor cell motility. *Cancer Cell* 2003; **4**: 67–79.
- Thuno M, Macho B, Eugen-Olsen J. suPAR: the molecular crystal ball. *Dis Markers* 2009; **27**: 157–172.
- Binder BR, Mihaly J, Prager GW. uPAR-uPA-PAI-1 interactions and signaling: a vascular biologist's view. *Thromb Haemost* 2007; **97**: 336–342.
- Sier CF, Stephens R, Bizik J, Mariani A, Bassan M, Pedersen N et al. The level of urokinase-type plasminogen activator receptor is increased in serum of ovarian cancer patients. *Cancer Res* 1998; **58**: 1843–1849.
- Stephens RW, Nielsen HJ, Christensen IJ, Thorlacius-Ussing O, Sørensen S, Danø K et al. Plasma urokinase receptor levels in patients with colorectal cancer: relationship to prognosis. *J Natl Cancer Inst* 1999; **91**: 869–874.
- Fernebro E, Madsen RR, Ferno M, Brønner N, Bendahl P, Christensen IJ et al. Prognostic importance of the soluble plasminogen activator receptor, suPAR, in plasma from rectal cancer patients. *Eur J Cancer* 2001; **37**: 486–491.
- Sorio C, Maffinci A, Furlan F, Barbi S, Bonora A, Brocco G et al. Elevated urinary levels of urokinase-type plasminogen activator receptor (uPAR) in pancreatic ductal adenocarcinoma identify a clinically high-risk group. *BMC Cancer* 2011; **11**: 448.
- Stahl A, Mueller BM. The urokinase-type plasminogen activator receptor, a GPI-linked protein, is localized in caveolae. *J Cell Biol* 1995; **129**: 335–344.
- Blasi F, Carmeliet P. uPAR: a versatile signalling orchestrator. *Nat Rev Mol Cell Biol* 2002; **3**: 932–943.
- Eugen-Olsen J, Gustafson P, Sidenius N, Fischer TK, Parner J, Aaby P et al. The serum level of soluble urokinase receptor is elevated in tuberculosis patients and predicts mortality during treatment: a community study from Guinea-Bissau. *Int J Tuberc Lung Dis* 2002; **6**: 686–692.
- Jo M, Thomas KS, Wu L, Gonias SL. Soluble urokinase-type plasminogen activator receptor inhibits cancer cell growth and invasion by direct urokinase-independent effects on cell signaling. *J Biol Chem* 2003; **278**: 46692–46698.
- Piccolella M, Festuccia C, Millimaggi D, Locatelli A, Bologna M, Motta M et al. suPAR, a soluble form of urokinase plasminogen activator receptor, inhibits human prostate cancer cell growth and invasion. *Int J Oncol* 2008; **32**: 185–191.
- Montuori N, Carriero MV, Salzano S, Rossi G, Ragno P. The cleavage of the urokinase receptor regulates its multiple functions. *J Biol Chem* 2002; **277**: 46932–46939.
- Furlan F, Orlando S, Laudanna C, Resnati M, Basso V, Blasi F et al. The soluble D2D3(88-274) fragment of the urokinase receptor inhibits monocyte chemotaxis and integrin-dependent cell adhesion. *J Cell Sci* 2004; **117**: 2909–2916.
- Myohanen HT, Stephens RW, Hedman K, Tapiovaara H, Rønne E, Hoyer-Hansen G et al. Distribution and lateral mobility of the urokinase-receptor complex at the cell surface. *J Histochem Cytochem* 1993; **41**: 1291–1301.
- Wei Y, Yang X, Liu Q, Wilkins JA, Chapman HA. A role for caveolin and the urokinase receptor in integrin-mediated adhesion and signaling. *J Cell Biol* 1999; **144**: 1285–1294.
- Wei Y, Eble JA, Wang Z, Kreidberg JA, Chapman HA. Urokinase receptors promote beta1 integrin function through interactions with integrin alpha3beta1. *Mol Biol Cell* 2001; **12**: 2975–2986.
- Kugler MC, Wei Y, Chapman HA. Urokinase receptor and integrin interactions. *Curr Pharm Des* 2003; **9**: 1565–1574.
- Ma Z, Thomas KS, Webb DJ, Moravec R, Salicioni AM, Mars WM et al. Regulation of Rac1 activation by the low density lipoprotein receptor-related protein. *J Cell Biol* 2002; **159**: 1061–1070.
- Giannini C, Sarkaria JN, Saito A, Uhm JH, Galanis E, Carlson BL et al. Patient tumor EGFR and PDGFR gene amplifications retained in an invasive intracranial xenograft model of glioblastoma multiforme. *Neuro-oncol* 2005; **7**: 164–176.
- Bagrodia S, Taylor SJ, Creasy CL, Chernoff J, Cerione RA. Identification of a mouse p21Cdc42/Rac activated kinase. *J Biol Chem* 1995; **270**: 22731–22737.



Oncogenesis is an open-access journal published by Nature Publishing Group. This work is licensed under a Creative Commons Attribution-NonCommercial-NoDerivs 3.0 Unported License. To view a copy of this license, visit <http://creativecommons.org/licenses/by-nc-nd/3.0/>

Supplementary Information accompanies this paper on the Oncogenesis website (<http://www.nature.com/oncsis>).